Heat capacity uncovers physics of a frustrated spin tube

Nedko B. Ivanov[1,2],*, Jürgen Schnack[2],†, Roman Schnalle[2], Johannes Richter[3], Paul Kögerler[4], Graham N. Newton[5], Leroy Cronin[5], Yugo Oshima[6], and Hiroyuki Nojiri[6‡]

[1]*Institute of Solid State Physics, Bulgarian Academy of Sciences, Tzarigradsko chaussee 72, 1784 Sofia, Bulgaria*
[2]*Fakultät für Physik, Universität Bielefeld, Postfach 100131, D-33501 Bielefeld, Germany*
[3]*Institut für Theoretische Physik, Universität Magdeburg, P.O. Box 4120, D-39016 Magdeburg, Germany*
[4]*Institut für Anorganische Chemie, RWTH Aachen, Landoltweg 1, D-52074 Aachen, Germany*
[5]*Dept. of Chemistry, The University of Glasgow, Glasgow, G12 8QQ, UK and*
[6]*Institute for Materials Research, Tohoku University, Katahira 2-1-1, Sendai 980-8577, Japan*
(Dated: April 15, 2010)

We report on refined experimental results concerning the low-temperature specific heat of the frustrated spin tube material $[(CuCl_2tachH)_3Cl]Cl_2$. This substance turns out to be an unusually perfect spin tube system which allows to study the physics of quasi-one dimensional antiferromagnetic structures in rather general terms. An analysis of the specific heat data demonstrates that at low enough temperatures the system exhibits a Tomonaga-Luttinger liquid behavior corresponding to an effective spin-3/2 antiferromagnetic Heisenberg chain with short-range exchange interactions. On the other hand, at somewhat elevated temperatures the composite spin structure of the chain is revealed through a Schottky-type peak in the specific heat located around 2 K. We argue that the dominating contribution to the peak originates from gapped magnon-type excitations related to the internal degrees of freedom of the rung spins.

Introduction–Spin tubes constitute a special class of quasi-one dimensional spin ladder systems characterized by periodic boundary conditions in the rung direction [1–13]. The magnetic compound $[(CuCl_2tachH)_3Cl]Cl_2$ is a geometrically frustrated triangular spin tube, the frustration being related both to the triangular arrangement of its rungs and to the twisted geometry of the legs, compare Fig. 1(a). The relatively simple exchange pathway structure, described only by two dominant Heisenberg exchange couplings [14, 15], as well as the extremely weak exchange interactions between neighboring tubes renders $[(CuCl_2tachH)_3Cl]Cl_2$ an excellent real material to study general properties of the spin-tube systems [5, 7, 10, 12, 16]. An appropriate spin Hamiltonian describing the magnetic properties of this material reads as

$$\mathcal{H} = \sum_{n=1}^{L}\sum_{\alpha=1}^{3}[J_1\,\boldsymbol{\sigma}_{n,\alpha}\cdot\boldsymbol{\sigma}_{n,\alpha+1} \qquad (1)$$
$$+ \ J_2\,\boldsymbol{\sigma}_{n,\alpha}\cdot(\boldsymbol{\sigma}_{n+1,\alpha+1}+\boldsymbol{\sigma}_{n+1,\alpha-1})]\ ,$$

where $\boldsymbol{\sigma}_{n,\alpha}$ ($\alpha = 1, 2, 3$) are spin-1/2 operators defined on the vertices of the elementary triangle denoted by index n ($n = 1, \ldots, L$). As depicted in Fig. 1 (b), the twisted spin tube may also be thought of as a three-leg ladder with periodic boundary conditions in the rung direction, where the parameters J_1 and J_2 are strengths of the rung and crossing (diagonal) exchange bonds, respectively. $[(CuCl_2tachH)_3Cl]Cl_2$ is characterized by the parameters $J_1/k_B = 1.8$ K and $J_2/k_B = 3.9$ K [15], whereas the leg exchange constant $J_2' > 0$, introduced for the sake of clarity in Fig. 1 (b), seems to vanish in

this material. Figure 1 (b) clearly reveals the translation symmetry with one triangle per unit cell.
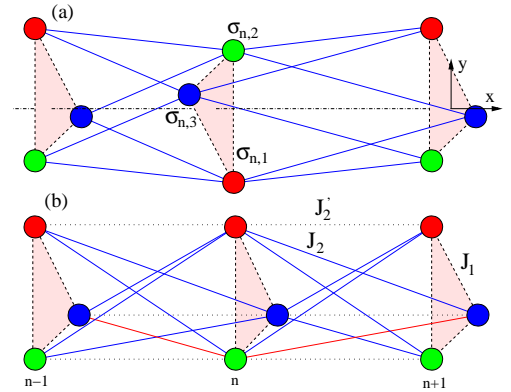

FIG. 1: (a) Sketch of the twisted spin-tube system. (b) An equivalent spin model obtained through inversion of every second triangle. The nth elementary cell contains the spin-1/2 operators $\boldsymbol{\sigma}_{n,1}, \boldsymbol{\sigma}_{n,2}$, and $\boldsymbol{\sigma}_{n,3}$.

Two extreme scenarios for the ground state of Eq. (1) with antiferromagnetic couplings $(J_1, J_2 > 0)$ were outlined in Ref. [10]. In the case of dominating J_1 couplings, the system effectively maps onto an effective spin-chirality model, where the additional chirality degrees of freedom appear as a result of the ground-state degeneracy of each individual triangle. On the other hand, for dominating J_2 couplings the system maps onto an effective spin-3/2 antiferromagnetic Heisenberg chain (AHC) containing additional biquadratic exchange couplings. In this Letter, we demonstrate by means of refined specific heat measurements, that the low-temperature proper-

ties of the spin tube material $[(CuCl_2tachH)_3Cl]Cl_2$ reproduce the behavior of a spin-3/2 AHC characterized by the effective short-range exchange coupling constant $J_{eff} = 2J_2/3$. Since the exchange interactions between different tubes are extremely small, the discussed compound also provides a rare example of spin-3/2 AHC [17–21]. The experimental observables strongly suggest that if the system ever orders this should be much below 0.1 K. At elevated temperatures the measured specific heat exhibits a big Schottky-type peak located around $T \approx 2$ K. A detailed analysis – combining the semiclassical spin-wave approach with a number of numerical techniques such as the Quantum Monte Carlo (QMC) method, the Lanczos exact numerical diagonalization (ED), and the complete exact diagonalization [22, 23] – implies that the main contribution to the specific-heat peak stems from the lowest-lying gapped magnon excitations resulting from the internal degrees of freedom of the composite rung spins.

For the following discussions it is instructive to rewrite Eq. (1) in the form

$$\mathcal{H} = \sum_{n=1}^{L} \left[\frac{J_1}{2} \left(\boldsymbol{s}_n^2 - \frac{9}{4} \right) + J_2\, \boldsymbol{s}_n \cdot \boldsymbol{s}_{n+1} \right] + V \ . \quad (2)$$

Here $\boldsymbol{s}_n = \boldsymbol{\sigma}_{n,1} + \boldsymbol{\sigma}_{n,2} + \boldsymbol{\sigma}_{n,3}$ is the rung spin operator related to the nth triangle. The number of Cu sites is $N = 3L$, where L is the number of rungs. The interaction term V reads as

$$V = (J_2' - J_2) \sum_{n=1}^{L} \sum_{\alpha=1}^{3} \boldsymbol{\sigma}_{n,\alpha} \cdot \boldsymbol{\sigma}_{n+1,\alpha} \ , \quad (3)$$

where we have included an additional leg exchange interaction J_2', see Fig. 1 (b). The last two equations explicitly show that the condition $J_2 = J_2'$ defines a special symmetric line in the parameter space on which the rung spin operators $\boldsymbol{s}_n$ are conserved quantities. On this line, the Hilbert space is decomposed into the invariant subspaces (sectors) $[s_1, s_2, \ldots, s_L]$, where the local spin quantum numbers $s_n = 1/2, 3/2$ are defined, as usual, by the relations $\boldsymbol{s}_n^2 = s_n(s_n + 1)$ $(n = 1, \ldots, L)$. In particular, if the Hamiltonian ground state lies in the sector $[3/2, 3/2, \ldots, 3/2]$, then Eq. (2) for $J_2 = J_2'$ will describe a spin-3/2 AHC characterized by the effective exchange constant $J_{eff} = J_2$. Up to first order in the (formally) small parameter $(J_2' - J_2)/J_1$, the effect of the interaction term V in Eq. (2) is reduced to a simple renormalization of the exchange constant in the effective spin-3/2 AHC: $J_{eff} \longrightarrow J_{eff} = J_2 + (J_2' - J_2)/3$. At the special point $J_2' = 0$, the result $J_{eff} = 2J_2/3$ coincides with the first-order result of Ref. [10], which is obtained by another perturbation scheme starting from the limit $|J_1| \gg J_2$ $(J_1 < 0)$.

Low-lying spin excitations–As argued below, the contributions to the low-temperature specific heat of the spin tube material $[(CuCl_2tachH)_3Cl]Cl_2$ are dominated by three types of low-lying spin excitations. Apart from the standard gapless excitations (characteristic of any half-integer AHC with short-range exchange couplings), important contributions to the specific heat appear from two additional branches of low-lying gapped magnon-type modes, which are related to the chirality degrees of freedom of the local triangles.

A qualitative picture of the low-lying spin excitations can be obtained already in the framework of the semiclassical spin-wave approach starting from the classical Néel configuration $|S_t, -S_t, \ldots\rangle$, where S_t is the maximal value of the z-component of the rung spin $(S_t = 3/2$ in the present case). Since the elementary cell contains three spin-S variables, there appear three different branches of spin-wave modes

$$E_m(k_x) = 4SJ_2 \times \qquad (4)$$
$$\sqrt{\left(1 - \alpha \sin^2 \frac{k_y}{2}\right)^2 - \frac{1}{4}\left[\cos k_x + \cos(k_x + k_y)\right]^2} \ ,$$

where $\alpha = J_1/J_2$, $k_y = 2\pi m/3$ $(m = 0, 1, 2)$, and S is the spin of a single site $(S = 1/2$ in the present case). As may be expected, the energy of the $m = 0$ branch does not depend on the parameter J_1, since it is related to the dynamics of the cell spins $\boldsymbol{s}_n$ as a whole:

$$E_0(k_x) = v_s |\sin k_x|, \qquad v_s = (6S)\frac{2J_2}{3} \ . \quad (5)$$

The above expressions reproduce the well-known semiclassical results for the dispersion relation and the related spin-wave velocity v_s of a spin-$(3 \cdot S)$ AHC with the effective exchange constant $J_{eff} = 2J_2/3$.
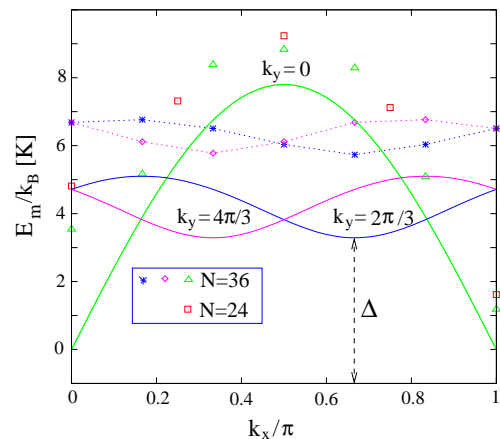

FIG. 2: Spin-wave excitation modes (solid curves, Eqs. (5) and (6)) compared with the lowest triplet excitations in two periodic clusters (symbols).

The dispersion relations of the $k_y = 2\pi/3$ and $k_y = 4\pi/3$ excitations can be expressed in the following form

$$E_{1,2}(k_x) = \sqrt{\Delta^2 + 4S^2 J_2^2 \sin^2\left(k_x \mp \frac{2\pi}{3}\right)} \ , \quad (6)$$

where the excitation gap $\Delta = 4SJ_2\sqrt{(1-3\alpha/4)^2 - 1/4}$ corresponds to the lowest-lying modes at wave vectors $k_x = \pi/3$ and $2\pi/3$.

The solid curves in Fig. 2 show the dispersion relations of the discussed spin-wave excitations. On the other hand, the symbols depict the positions of the lowest-lying triplet states, as obtained by the ED method for periodic clusters containing $L = 8$ and 12 unit cells [27]. Apart from the finite-size effects related to the ED results, it is clearly seen that both methods qualitatively yield similar results. As a matter of fact, the discussed spin-wave branches may also be considered as one-dimensional analogs of the three spin-wave branches in the triangular lattice antiferromagnet. In this respect, the lowest-lying excitations at $k_x = 0, 2\pi/3$ and $4\pi/3$ in the spin tube are one-dimensional analogs of the three Goldstone modes in the triangular lattice antiferromagnet.

More accurate estimates for the parameters of the excitation spectrum v_s and Δ can be obtained from an extrapolation of the ED results for $L = 6, 8, 10,$ and 12 unit cells. Using the approach of Ref. [18], one finds the following estimates from the extrapolations of $E_0(2\pi/L)$ vs. $\sin(2\pi/L)/L$ and $E_1(2\pi/3)$ vs. $1/L$ (see Fig. 3):

$$v_s/k_B = 10.06\,\text{K} = 3.87\frac{2J_2}{3k_B} \ , \ \ \Delta/k_B = 5.32\,\text{K} \ . \quad (7)$$

Interestingly, the extrapolation result $3v_s/(2J_2) = 3.87$ exactly reproduces the density-matrix renormalization group estimate for the spin-wave velocity of the spin-3/2 AHC characterized by the exchange constant $2J_2/3$ [18]. As already discussed, the same effective exchange constant $(J_{\text{eff}} = 2J_2/3)$ arises both in the first-order result for the effective spin model and in the semiclassical spin-wave approach. Below we demonstrate numerically that the specific heat of a spin-3/2 AHC with the exchange constant $2J_2/3$ excellently reproduces the experimental results in the low-temperature region $T \leq 0.5$ K.
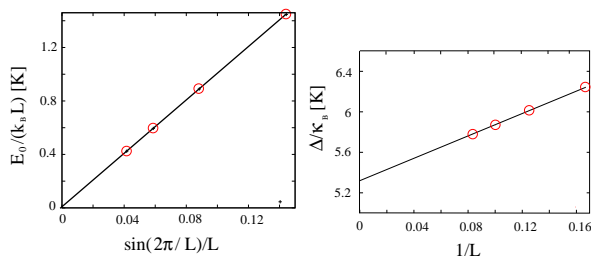

FIG. 3: Extrapolation of the ED results giving the parameters of the excitation spectrum v_s (l.h.s.) and Δ (r.h.s.).

Low-temperature specific heat–The specific heat, Figs. 4 and 5, was measured at the Institute for Materials Research (IMR) of Tohoku University using polycrystalline samples of the spin tube material $[(CuCl_2tachH)_3Cl]Cl_2$. The solid curve in Fig. 4 depicts the specific heat of a spin-3/2 periodic AHC composed of 100 spin sites. The specific heat is evaluated by means of a QMC method employing the ALPS code [24]. As an effective exchange parameter we used $J_{\text{eff}} = 2J_2/3$. As can be seen in Fig. 4, the QMC result reproduces the experimental data very well in the region $T \leq 0.5$. This means that even for $J_2' = 0$, when the parameter $(J_2' - J_2)$ is definitely not small, the low-energy physics of Hamiltonian (1) is described by the spin-3/2 AHC. Therefore, it turns out that the theoretically predicted biquadratic exchange term [3, 10] plays no role in the experimentally interesting region of the phase diagram characterized by the dimensionless parameter $J_1/J_2 = 0.46$.
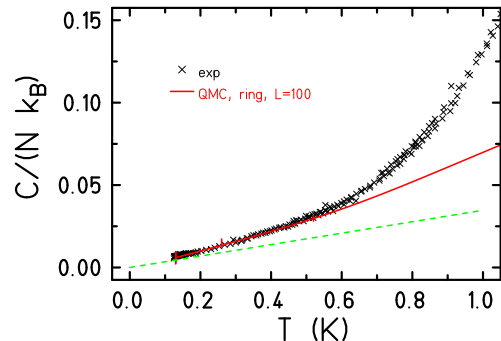

FIG. 4: Specific heat (per Cu spin) of $[(CuCl_2tachH)_3Cl]Cl_2$. The symbols denote the experimental values. The solid curve is the QMC result for a spin-3/2 chain of length $L = 100$. The dashed line provides the linear specific heat corresponding to the universal Tomonaga-Luttinger liquid form presented by Eq. (8), by using the extrapolation result $v_s = 10.06$ K.

Turning to the extremely low-temperature regime, we expect the universal specific-heat behavior of the Tomonaga-Luttinger liquid

$$\frac{C(T)}{Nk_B} = \frac{\pi c T}{9v_s} \ , \quad (8)$$

where the constant c stands for the so-called topological charge ($c = 1$ for a Tomonaga-Luttinger liquid state) and v_s is the velocity of the gapless spin excitations. As clearly seen in Fig. 4, already for $T \leq 0.5$ K the measured specific heat coincides with the QMC results and nicely extrapolates towards the universal behavior repesented by Eq. (8). The latter observations strongly imply that the spin tube compound $[(CuCl_2tachH)_3Cl]Cl_2$ is characterized by a gapless Tomonaga-Luttinger liquid ground state. In a recent report, Nuclear Magnetic Resonance measurements also indicate a gapless spin state in the same material based on estimates for the extremely low-temperature part of the magnetic susceptibility [25].

To explain the experimental data at intermediate temperatures around 2 K, we use the established structure of the low-lying excitation spectrum, compare Fig. 2. As a rough approximation, one may take $E_{1,2}(k_x) \approx \Delta$ and use the well-known expression for the specific heat of a two-level system (with the assumption that the excited

level has twice the weight of the ground state, i.e., $r = 2$ in the following expression). Since the exact density of states is not known in the thermodynamic limit, we use an overall parameter A in order to fix the height of the Schottky peak:

$$\frac{C}{Nk_B} = A \frac{r(\Delta/T)^2 \exp(\Delta/T)}{[\exp(\Delta/T) + r]^2} \ . \tag{9}$$

Notice that the position of the peak does not depend on the value of A. The expression for $C(T)$, Eq. (9), with $\Delta/k_B = 5.32$ K is plotted in Fig. 5 by a thick curve together with the experimental data. One observes that it reproduces very well not only the position of the peak ($T_m \approx 2$ K) but also the behavior of the specific heat for $T < T_m$ down to $T \approx 0.7$ K, where the contribution from the gapless branch $E_0(k_x)$ becomes important. In addition, in Fig. 5 we also show the specific heat that results from complete diagonalizations of a few finite-size periodic clusters. As easily seen, the overall agreement is good, in spite of the pronounced finite-size effects.
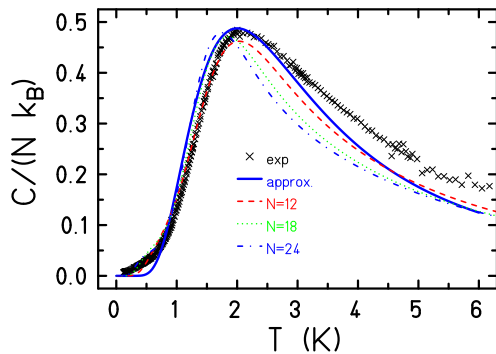

FIG. 5: Specific heat (per Cu spin) of $[(CuCl_2tachH)_3Cl]Cl_2$. The symbols denote the experimental values, whereas the solid curve depicts the two-level approximation. The broken curves denote the specific heat for three complete diagonalizations for finite sizes.

Turning to higher temperatures, a few words are necessary to expain the discrepancies between the experimental and numerical results for $C(T)$. Notice that already at $T \approx 2$ K the phonon contribution begins to dominate the specific heat. Since the detailed phonon spectral density is unknown, the raw experimental data for $C(T)$ was – as usually – corrected by subtracting a reasonable Debye-like specific heat contribution [26].

Conclusion–We demonstrated that the low-temperature specific heat behavior of the spin tube compound $[(CuCl_2tachH)_3Cl]Cl_2$ suggests a Tomonaga-Luttinger liquid type ground state for this material, corresponding to an effective spin-3/2 antiferromagnetic Heisenberg chain characterized by the short-ranged exchange-coupling constant $J_{eff} = 2J_2/3$. On the other hand, we argued that the main contribution to the observed Schottky-type peak around $T \approx 2$ K comes from the lowest-lying gapped magnon-type excitations resulting from the internal degrees of freedom of the composite rung spins.

* Electronic address: ¡Nedko.Ivanov@Physik.Uni-Magdeburg.DE¿
† Electronic address: jschnack@uni-bielefeld.de
‡ Electronic address: nojiri@imr.tohoku.ac.jp
[1] P. Millet, J. Y. Henry, F. Mila, and J. Galy, J. Solid State Chem. **147**, 676 (1999).
[2] J. L. Gavilano, D. Rau, S. Mushkolaj, H. R. Ott, P. Millet, and F. Mila, Phys. Rev. Lett. **90**, 167202 (2003).
[3] A. Lüscher, R. M. Noack, G. Misguich, V. N. Kotov, and F. Mila, Phys. Rev. B **70**, 060405(R) (2004).
[4] M. Sato, J. Phys. Chem. Solids **66**, 1454 (2005).
[5] M. Sato, Phys. Rev. B **72**, 104438 (2005).
[6] M. Matsumoto, T. Sakai, M. Sato, H. Takayama, and S. Todo, Physica E **29**, 660 (2005).
[7] T. Sakai, M. Matsumoto, K. Okunishi, K. Okamoto, and M. Sato, Physica E **29**, 633 (2005).
[8] T. Saha-Dasgupta, R. Valentí, F. Capraro, and C. Gros, Phys. Rev. Lett. **95**, 107201 (2005).
[9] K. Okunishi, S. Yoshikawa, T. Sakai, and S. Miyashita, Prog. Theor. Phys. Suppl. **159**, 297 (2005).
[10] J.-B. Fouet, A. Läuchli, S. Pilgram, R. M. Noack, and F. Mila, Phys. Rev. B **73**, 014409 (2006).
[11] M. Sato and T. Sakai, Phys. Rev. B **75**, 014411 (2007).
[12] S. Nishimoto and M. Arikawa, Phys. Rev. B **78**, 054421 (2008).
[13] O. Zaharko, J. L. Gavilano, T. Strässle, C. F. Miclea, A. C. Mota, Y. Filinchuk, D. Chernyshov, P. P. Deen, B. Rahaman, T. Saha-Dasgupta, et al., Phys. Rev. B **78**, 214426 (2008).
[14] G. Seeber, P. Kögerler, B. M. Kariuki, and L. Cronin, Chem. Commun. pp. 1580–1581 (2004).
[15] J. Schnack, H. Nojiri, P. Kögerler, G. J. T. Cooper, and L. Cronin, Phys. Rev. B **70**, 174420 (2004).
[16] J. Schnack, C. R. Chimie **10**, 15 (2007).
[17] T. Xiang, Phys. Rev. B **58**, 9142 (1998).
[18] K. Hallberg, X. Q. G. Wang, P. Horsch, and A. Moreo, Phys. Rev. Lett. **76**, 4955 (1996).
[19] A. Klümper and D. C. Johnston, Phys. Rev. Lett. **84**, 4701 (2000).
[20] D. C. Johnston, R. K. Kremer, M. Troyer, X. Wang, A. Klümper, S. L. Bud'ko, A. F. Panchula, and P. C. Canfield, Phys. Rev. B **61**, 9558 (2000).
[21] S. Itoh, Y. Endoh, K. Kakurai, H. Tanaka, S. M. Bennington, T. G. Perring, K. Ohoyama, M. J. Harris,

K. Nakajima, and C. D. Frost, Phys. Rev. B **59**, 14406 (1999).

[22] J. Schnack, P. Hage, and H.-J. Schmidt, J. Comput. Phys. **227**, 4512 (2008).

[23] R. Schnalle and J. Schnack, Phys. Rev. B **79**, 104419 (2009).

[24] A. Albuquerque, F. Alet, P. Corboz, P. Dayal, A. Feiguin, S. Fuchs, L. Gamper, E. Gull, S. Gürtler, A. Honecker, et al. (ALPS collaboration), J. Magn. Magn. Mater. **310**, 1187 (2007).

[25] Y. Furukawa, Y. Sumida, K. Kumagai, H. Nojiri, P. Kögerler, and L. Cronin, J. Phys. Conf. Ser. **150**, 042036 (2009).

[26] S. Yamashita, Y. Nakazawa, M. Oguni, Y. Oshima, H. Nojiri, Y. Shimizu, K. Miyagawa, and K. Kanoda, Nat. Phys. **4**, 459 (2008).

[27] Apart from the discussed two branches of gapped triplet modes, there are two additional branches of gapped singlet modes also related to the chirality degrees of freedom of the local triangles. However, in the experimentally interesting region of the phase diagram ($J_1/J_2 = 0.46$) these singlet modes lie above the triplet excitations presented in Fig. 2.